

POURBAIX DIAGRAMS FOR URANIUM, MOLYBDENUM and TECHNETIUM

W.T. Thompson*, B.J. Lewis, C. Morrison, M. Webb and F. Akbari
Department of Chemistry and Chemical Engineering,
Royal Military College of Canada
PO Box 17000, Kingston, Ontario K7K 7B4

ABSTRACT

Pourbaix diagrams represent in redox potential – pH space the isothermal phase equilibrium of a particular element in contact with water. The phase equilibrium involving aqueous ions or complex ions potentially coexisting with solid oxides or hydrated oxides is essential in understanding fuel behaviour in direct contact with water. The treatment will describe a method of constructing the diagrams by Gibbs energy minimization, highlight the significant features of the diagrams, and show how the data may be used in support of a mass transport model.

Recent modelling activity in our laboratory has put emphasis on high temperature equilibrium involving UO_2 with noble metal fission products. Under lower temperature conditions, defective fuel may come into direct contact with the water phase. The chemical consequences require the introduction of aqueous ions into the computations. The data must be consistent with that for the solid oxide phases used in the U-O temperature-composition phase diagram development. A good test of self-consistency is the generation of the Pourbaix diagram for that element. The presentation will show how these diagrams may be developed by means that do not require an *a priori* knowledge of adjacent phases or domains. The technique of Gibbs energy minimization will be illustrated with graphical and tabular displays of the steps in this versatile approach. The presentation will conclude by showing how the data may be blended together to understand the boundary condition in the transport of Mo and Tc from defective fuel into the primary heat transfer system.

1. INTRODUCTION

Redox potential, E_h , and pH are among the most important variables in understanding the thermodynamics of a particular element in water. Accordingly the phase diagrams for 298.15 K devised and published by Pourbaix¹ have developed a high standing in such fields of applied chemistry as corrosion, hydrometallurgy, and battery technology. The same diagrams, perhaps adjusted for temperature, have application in mass transport modelling of fission products from fuel when conditions of temperature and pressure are such that H_2O (or D_2O) can contact UO_2 as a liquid. The solubilities of metallic ions or complex ions and the speciation is of interest as a boundary condition.

The original development of the Pourbaix diagrams put emphasis on the species and phases that could coexist as a preliminary to formulating equilibrium expressions in terms of E_h and pH in order to place phase boundaries. This approach² is useful in developing an understanding of Pourbaix diagrams but is no longer a necessary (or even advisable) basis for construction. Gibbs energy minimization considers all the candidate chemical species of a particular element (eg., U) potentially dissolved (eg., UO_2^{2+} , ..) or in contact with water (eg., U_4O_9 , ..) and does not involve “a priori” knowledge of particular equilibria. The minimization procedure in effect finds the relevant equilibria by objective means thereby enabling rapid reliable construction of the diagram at any temperature of interest as revised or additional data is acquired.

2. GIBBS ENERGY MINIMIZATION

This computational technique will be illustrated here for uranium. The cornerstone concept is to express the formation of all possible U-H-O species from a mole of U in its most stable allotropic form (oC4) at the temperature in question. The formation reactions are balanced using only H₂O, H⁺ and e⁻. These reactions are listed in Table 1 with the standard Gibbs energy changes (that is, at E_h(S.H.E.) = 0, pH = 0, molality (activity) ions = 1) for 298.15 and 373.15 K. To build the diagram over the desired range of E_h and pH, adjustments are made to the standard Gibbs energies in Table 1 to reflect departure from the standard state condition. The steps in the incremental changes of E_h and pH are conveniently made the same as each pixel in the display. At each step, the Gibbs energies in Table 1 are adjusted by the addition of the following:

$$\Delta G_{\text{H}^+} = -2.303 R T \text{ pH} \quad (1)$$

$$\Delta G_{\text{e}^-} = -\mathfrak{F} E_{\text{h}} \quad (2)$$

In the treatment of the “electron”, it must be remembered that “e⁻” is actually a notation representative of another unspecified process in the water phase that controls the redox potential, for example, dissolved oxygen:



When equation (2) is used one is in effect finding the Gibbs energy change for a process such as (3) for some particular dissolved oxygen concentration, which determines E_h at a specified pH and temperature. Pourbaix diagrams generally show the influence of concentration of aqueous species, which has the effect of enlarging the aqueous domains as dilution increases. This aspect of diagram development simply involves adjusting the Gibbs energies in Table 1 (per mole of U-containing ion) by (R T ln m) where m is molality (activity). With all Gibbs energies in Table 1 adjusted for concentration, E_h and pH, the lowest value is then found. This identifies the particular U-containing species that is most stable. By repetition of this process for each point (pixel) on the diagram (display), the domains of the different species (colours) can be established. Computing time is saved by realizing that domains must be contiguous enabling the computation of even a quite complex diagram in a second or two or real time.

3. POURBAIX DIAGRAMS FOR URANIUM

The Uranium Pourbaix diagram at 298.15 K covering the range of redox potential pertinent to fuel oxidation is shown in Fig. 1 (a) and (b). The data for UO₂, U₄O₉, U₃O₇ and U₃O₈ is the same as that used for the U-O binary phase diagram³. Placed on the diagram for reference are dashed lines (a) and (b) corresponding to redox potentials associated with hydrogen and oxygen saturation (at 1 atm.) respectively.

The origin of Fig. 1(a) and (b) provides a simple check of the foregoing Gibbs energy minimization, since there is no need to make any Gibbs energy adjustment to Table 1. The species UOH³⁺ with the lowest Gibbs energy change is indeed dominant on the Pourbaix diagram at E_h=0 and pH = 0.

Since the Gibbs energy changes for the reactions in Table 1 vary linearly with E_h and pH, each species in Table 1 can be associated with a plane in ΔG – E_h –pH space. The envelope of lowest planes viewed normal to E_h-pH plane provides the Pourbaix diagram for the fixed concentration that applies to each

aqueous species. This is illustrated in Fig. 2, which can be related to the domains on the Pourbaix diagram in Fig. 1(a) and (b) at 10^{-6} m.

The effect of raising the temperature to 373.15 K for the uranium Pourbaix diagram is shown in Fig. 3 (a) and (b).

4. POURBAIX DIAGRAMS FOR MOLYBDENUM AND TECHNETIUM

These diagrams are of interest in connection with fission product leaching of defective fuel elements during reactor shutdown operations⁴. In the case of Mo, the data yielding the diagrams in Figs 4 and 5 are shown in Table 2⁵.

The diagrams for Tc are developed from the Gibbs energies in Table 3. The Gibbs energy changes for TcO_2 and TcO_4 incorporate the data of Lemire and Jobe⁶. Under strongly acid conditions it appears that neutral HTcO_4 can develop. The dissociation constant for



is believed to be near unity so the properties for HTcO_4 were adjusted to be consistent with Lemire and Jobe⁶. The diagrams shown in Figs. 6 and 7 have been deliberately projected to unrealistically low pH in order to make more evident the features of the Tc^{2+} field, which barely reaches a pH of zero at either temperature. The greater stability of TcO_2 ⁶ has the effect of eliminating the TcO_3 phase as a stable phase from the diagram. Also note as a point of connection with Table 3 that the Tc metal field covers the area near $E_h = 0$ and $\text{pH} = 0$ since the standard Gibbs energies of all other Tc species are positive.

5. APPLICATION OF POURBAIX DIAGRAMS

The Pourbaix diagrams can now be brought to bear on the leaching Mo and/or Tc fission products from UO_2 fuel. Mo and Tc are principally found in association with Ru, Rh, and Pd in metallic inclusions in spent or partially burned fuel. Since UO_2 is by far the dominant solid phase, the redox potential of the water will eventually be controlled by the UO_2 water reactions. Fig. 8 shows the most stable species from among all of those associated with Table 1 when 1 mole of UO_2 reaches an equilibrium in 1 kg (55.5 moles) of H_2O at 298.15 K. The computation, based on Gibbs energy minimization^{7,8} with data in Table 1, is truncated at concentrations (activities) of 10^{-10} m. This result is in keeping with Fig. 1. The computed redox potential (-0.201 volt (SHE)) and pH (7.003) in Fig. 8 locates a point in the field of UO_2 on Fig. 1 where the concentration of the most populous ion, UO_2^+ is well below 10^{-6} m.

The disposition of Mo and Tc can now be understood using the Pourbaix diagrams since the appropriate E_h and pH have been determined. Mo is oxidized principally to MoO_4^{2-} ions. Because of the proximity to the HMoO_4^- domain this species would be the next most populous ion. The distance from the Mo^{3+} domain indicates that the concentration of this ion would likely be below detection. The solid oxide MoO_3 is very unstable. The oxide MoO_2 might be found as an unstable intermediate during the course of Mo (metal) becoming MoO_4^{2-} . In the case of Tc, the redox potential and pH associated with Fig. 8, places a point on or near the Tc/ TcO_2 phase boundary. With the Lemire and Jobe data for TcO_2 ⁶, this is the more stable phase. With other data⁵, Tc remains unoxidized. In any event, conditions are far away from detectable concentrations of aqueous species TcO_4^- , HTcO_4 or Tc^{2+} . All of this implies that if Tc were detected in the water phase, it could only arise (in the absence of dissolved oxygen) as a result of the decay of Mo, which the Pourbaix diagram advises has indicated is easily leached. If air were allowed to come into contact with the water phase (as might be the case in storage of spent fuel), the redox potential

would slowly rise as UO_2 is converted initially to U_4O_9 but even at this higher potential conditions are such that TcO_2 is still virtually insoluble.

6. CONCLUSION

Pourbaix diagrams, made consistent with other relevant thermodynamic data, are a useful way to develop an overview of the aqueous chemistry of elements important in nuclear fuel technology.

In particular, they draw attention to the sometimes overlooked role of redox potential in controlling the speciation and preferred phase of a particular element. The diagrams can be rapidly constructed by Gibbs energy minimization enabling customizing of the diagrams for particular applications that fall outside the scope of those gathered in standard compilations.

7. ACKNOWLEDGEMENT

The authors acknowledge the support of the Natural Sciences and Engineering Research Council of Canada

8. REFERENCES

- 1) M. Pourbaix, "Atlas of Electrochemical Equilibria in Aqueous Solutions", Pergamon, New York, 1966
- 2) E.D. Verink, "Simplified Procedure for Constructing Pourbaix Diagrams", Uhlig's Corrosion Handbook, Second Edition, R.W. Revie Editor, John Wiley and Sons, Inc., 2000
- 3) D.M. Thompson, B.J. Lewis, F. Akbari and W.T. Thompson "Part I: Thermodynamics of Uranium Oxidation in Support of Kinetics Model for Operating Defective Fuel Elements", 8th International Conference on CANDU Fuel, Honey Harbour, Ontario, Canada, Sept. 21-24, 2003
- 4) B.J. Lewis, W.T. Thompson and A. Husain, "Modelling Activity of ⁹⁹Tc in the Primary Heat Transport System of a CANDU Reactor", 8th International Conference on CANDU Fuel, Honey Harbour, Ontario, Canada, Sept. 21-24, 2003
- 5) C.W. Bale, A.D. Pelton and W.T. Thompson, "Facility for the Analysis of Chemical Thermodynamics", Ecole Polytechnique de Montreal, 2002
- 6) R. J. Lemire and D. J. Jobe, "predicted behaviour of Technetium in a Geological Disposal Vault for Used Nuclear Fuel-Ramifications of a Recent Determination of the Enthalpy of Formation of TcO_2 ", Materials Research Society Symposium Proceedings, Vol. 412, 1996, pp. 873-880, Materials Research Society
- 7) G. Eriksson and W.T. Thompson, "A Procedure to Estimate Equilibrium Concentrations in Multicomponent Systems and Related Applications", CALPHAD, Vol 13, No. 4, pp 389-400, 1989
- 8) G. Eriksson, "SOLGASMIX Gibbs Energy Minimization Program", Chemica Scripta, Vol. 8, p. 100, 1975

Table 1: Formation of Uranium Compounds and Associated Changes in Standard Gibbs Energy (ΔG°)(J/mol)

Reaction	T = 298.15 K	T = 373.15 K
$U_{(s)} \rightarrow U_{(s1)}$	0	0
$U_{(s1)} \rightarrow U_{(s2)}$	1899.9	1685.3
$U_{(s1)} \rightarrow U_{(s3)}$	3914	3966.1
$U_{(s1)} \rightarrow U_{(l)}$	6172.1	10197.1
$U_{(s1)} \rightarrow U_{(g)}$	453513.4	445041.8
$U_{(s1)} \rightarrow U^{3+}_{(aq)} + 3e^-$	-520616.3	-521598.8
$U_{(s1)} \rightarrow U^{4+}_{(aq)} + 4e^-$	-531821.3	-516466.5
$U_{(s1)} + 3H^+ + 3e^- \rightarrow UH_3(s)$	-72773.1	-58882.3
$U_{(s1)} + H_2O_{(l)} \rightarrow UO_{(g)} + 2H^+ + 2e^-$	252146.1	233103.8
$U_{(s1)} + 2H_2O_{(l)} \rightarrow UO_{2(s)} + 4H^+ + 4e^-$	-557615.5	-568289.3
$U_{(s1)} + 2 H_2O_{(l)} \rightarrow UO_{2(g)} + 4H^+ + 4e^-$	3336.2	-21627.2
$U_{(s1)} + 2H_2O_{(l)} \rightarrow UO_2^{+}_{(aq)} + 4H^+ + 5e^-$	-519894.8	-533365.9
$U_{(s1)} + 2 H_2O_{(l)} \rightarrow UO_2^{2+}_{(aq)} + 4H^+ + 6e^-$	-514898.7	-523925.2
$U_{(s1)} + 3 H_2O_{(l)} \rightarrow UO_{3(g)} + 6H^+ + 6e^-$	-70484.6	-102603.3
$U_{(s1)} + H_2O_{(l)} \rightarrow UOH_{(g)} + H^+ + e^-$	307110.7	291116.4
$U_{(s1)} + H_2O_{(l)} \rightarrow UOH^{3+}_{(aq)} + H^+ + 4e^-$	-572299.7	-572410.3
$U_{(s1)} + 2 H_2O_{(l)} \rightarrow UO_2H_{2(g)} + 2H^+ + 2e^-$	145653.4	125335.3
$U_{(s1)} + 2 H_2O_{(l)} \rightarrow H_2O_2U^{2+}_{(aq)} + 2H^+ + 4e^-$	-516616.6	-515685.3
$U_{(s1)} + 3 H_2O_{(l)} \rightarrow HO_3U^{+}_{(aq)} + 5H^+ + 6e^-$	-445431.2	-455587.3
$U_{(s1)} + 3 H_2O_{(l)} \rightarrow H_3O_3U^{+}_{(aq)} + 3H^+ + 4e^-$	721535.9	-499888.6
$U_{(s1)} + 4 H_2O_{(l)} \rightarrow UO_3(H_2O)_{(s)} + 6H^+ + 6e^-$	-452724.2	-466359.9
$U_{(s1)} + 4 H_2O_{(l)} \rightarrow UO_3(H_2O)_{(g)} + 6H^+ + 6e^-$	121398.8	-216427.4
$U_{(s1)} + 5 H_2O_{(l)} \rightarrow UO_3(H_2O)_{2(s)} + 6H^+ + 6e^-$	-450988.2	-463283.1
$U_{(s1)} + 5 H_2O_{(l)} \rightarrow U(OH)_5^{-}_{(aq)} + 5H^+ + 4e^-$	-444786.4	-435190.9
$U_{(s1)} + 3 H_2O_{(l)} \rightarrow 1/2H_2O_6U_2^{2+}_{(aq)} + 5H^+ + 6e^-$	-462436.1	-469939.75
$U_{(s1)} + 11/3 H_2O_{(l)} \rightarrow 1/3H_5O_{11}U_3^{+}_{(aq)} + 17/3H^+ + 18/3e^-$	-448733.1	-456009.267
$U_{(s1)} + 13/3 H_2O_{(l)} \rightarrow 1/3(UO_2)_3(OH)_7^{-}_{(aq)} + 19/3H^+ + 18/3e^-$	-419888.6	-430324.667
$U_{(s1)} + 3 H_2O_{(l)} \rightarrow UO_3(s) + 6H^+ + 6e^-$	-434199.5	-450537.4
$U_{(s1)} + 7/3 H_2O_{(l)} \rightarrow 1/3U_3O_7(s) + 14/3H^+ + 14/3e^-$	-526605	-539375.033
$U_{(s1)} + 8/3 H_2O_{(l)} \rightarrow U_3O_8(s) + 16/3H^+ + 16/3e^-$	-490250.8	-505044.667
$U_{(s1)} + 9/4 H_2O_{(l)} \rightarrow 1/4U_4O_9(s) + 18/4H^+ + 18/4e^-$	-535375.9	-547594.45

Table 2: Gibbs Energy Changes for Mo species (kJ/mol)

Reaction	298.15 K	373.15K
Mo = Mo	0	0
Mo = Mo ⁺³ + 3e ⁻	-57.86	-48.31
Mo + 2H ₂ O = MoO ₂ + 4H ⁺ + 4e ⁻	-57.63	-67.60
Mo + 3H ₂ O = MoO ₃ + 6H ⁺ + 6e ⁻	-11.34	-27.98
Mo + 4H ₂ O = MoO ₄ ⁻² + 8H ⁺ + 6e ⁻	43.50	38.86
Mo + 4H ₂ O = HMoO ₄ ⁻ + 7H ⁺ + 6e ⁻	10.42	5.78

Table 3: Gibbs Energy Changes for Tc species (kJ/mol)

Reaction	298.15 K	373.15 K
Tc = Tc	0	0
Tc = Tc ⁺² + 2e ⁻	71.93	69.33
Tc + 2H ₂ O = TcO ₂ + 4H ⁺ + 4e ⁻	69.58	60.23 ⁶
Tc + 3H ₂ O = TcO ₃ + 6H ⁺ + 6e ⁻	252.35	236.31
Tc + 4H ₂ O = TcO ₄ ⁻ + 8H ⁺ + 7e ⁻	311.4	287.52 ⁶
Tc + 4H ₂ O = HTcO ₄ + 7H ⁺ + 7e ⁻	311.4	287.52 ⁶

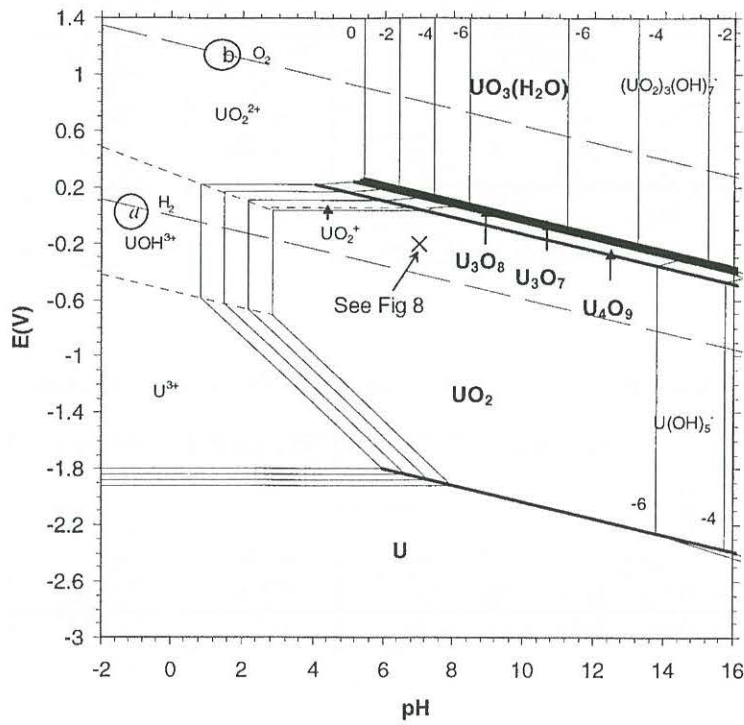


Fig. 1(a): F.A.C.T generated U-H₂O Pourbaix diagram at 298.15 K

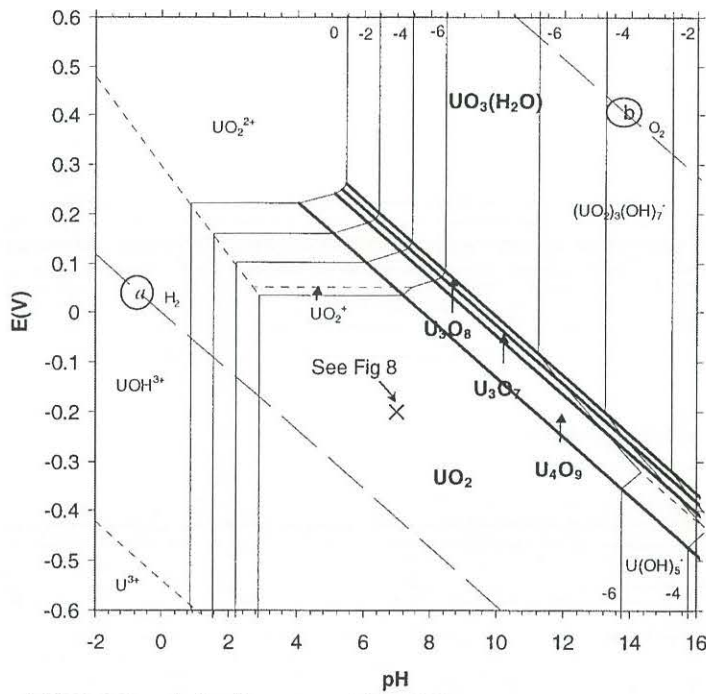


Fig. 1(b): F.A.C.T generated U-H₂O Pourbaix diagram at 298.15 K

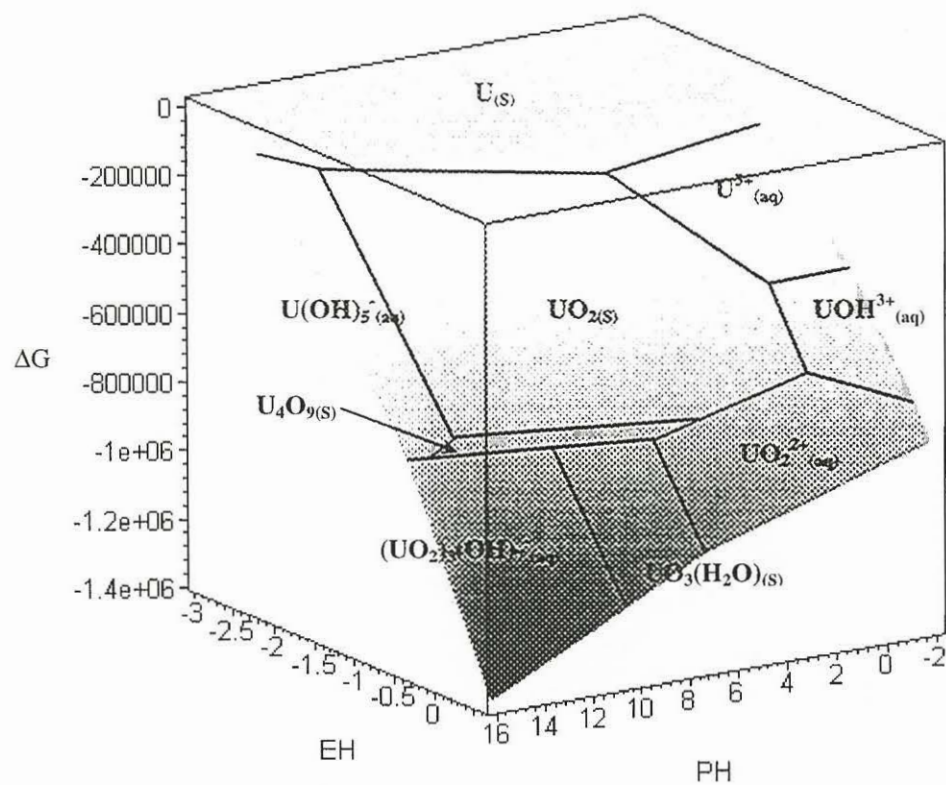


Fig. 2: The minimum surface of values for changes in Gibbs Energy for all U-OH compounds in an aqueous system at 298.15 K and concentration of 10^{-6} molal. The Figure has been simplified in the area near U_4O_9 .

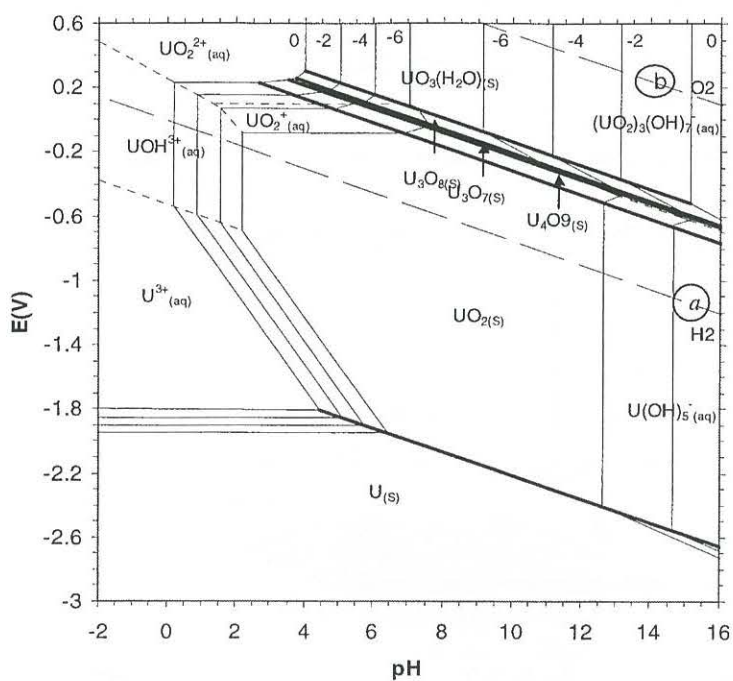


Fig. 3(a): F.A.C.T generated U-H₂O Pourbaix diagram at 373.15 K

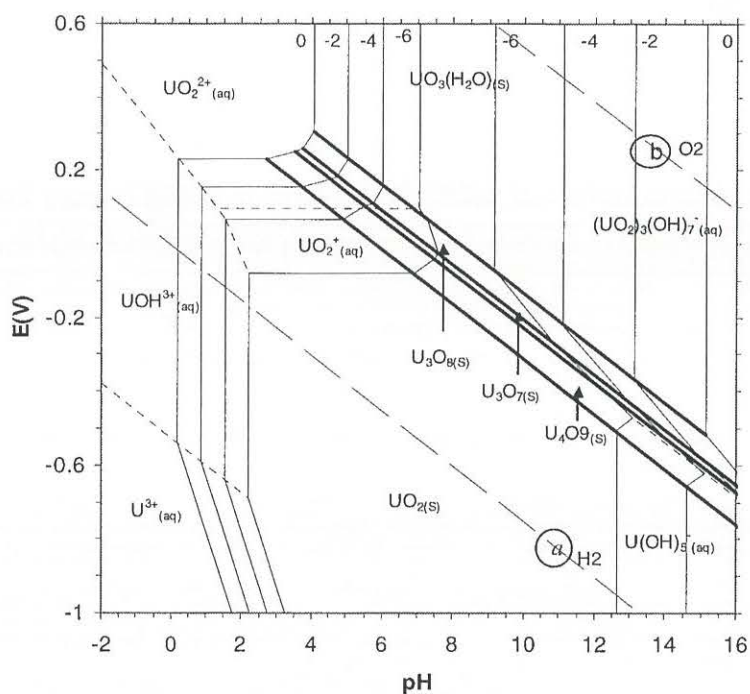


Fig. 3(b): F.A.C.T generated U-H₂O Pourbaix diagram at 373.15 K

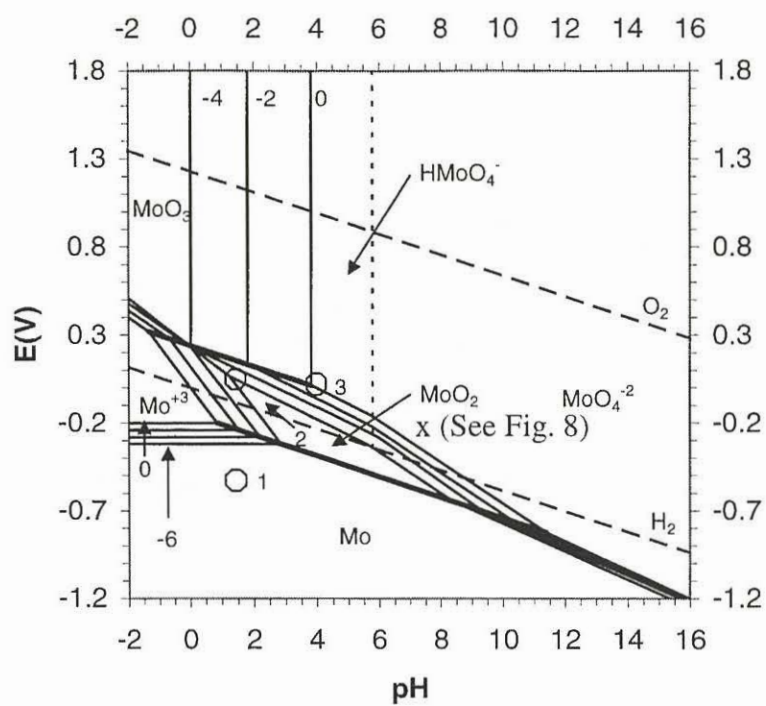


Fig. 4: F.A.C.T generated Mo-H₂O Pourbaix diagram at 298.15 K

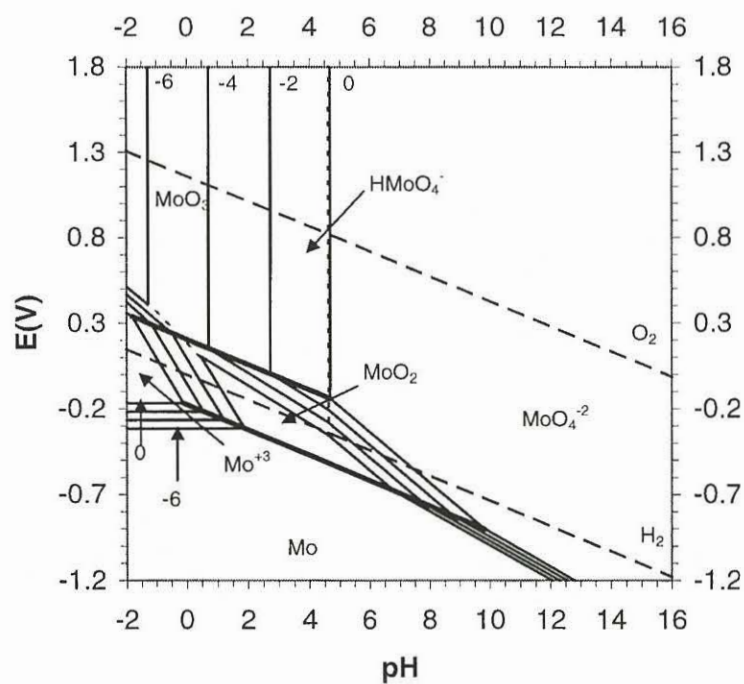


Fig. 5: F.A.C.T generated Mo-H₂O Pourbaix diagram at 373.15 K

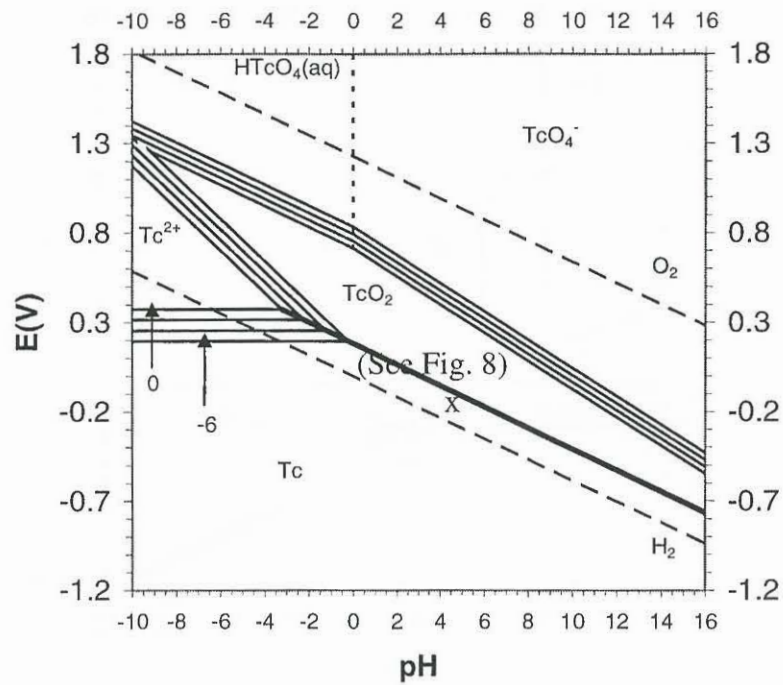


Fig. 6: F.A.C.T generated Tc-H₂O Pourbaix diagram at 298.15 K

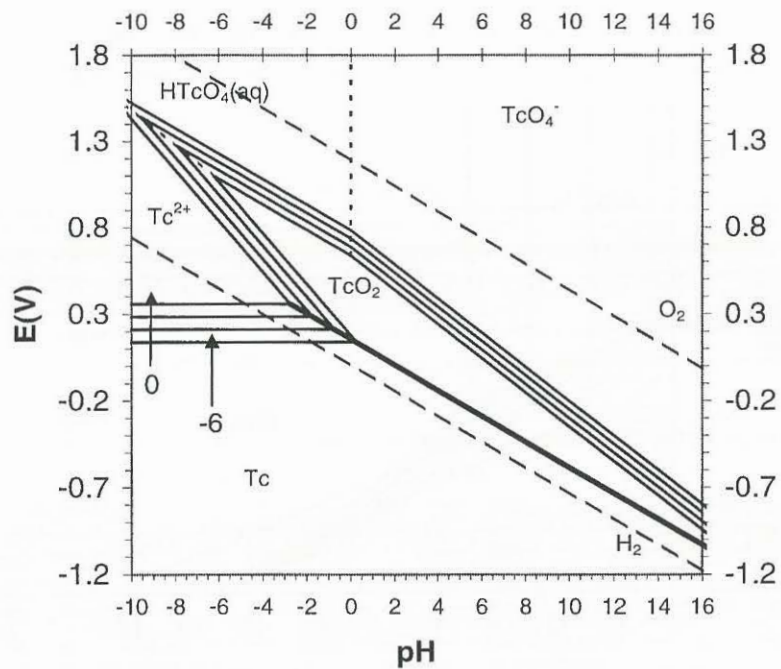


Fig. 7: F.A.C.T generated Tc-H₂O Pourbaix diagram at 373.15 K

55.5 H₂O + UO₂ =

```

0.00000 mol ( 0.31352E-01 H2O
              + 0.59256E-07 H2)
              ( 298.15 K, 1.0000 atm, gas_ideal, a=0.31353E-01)

+ 0.99986 mol ( 55.508 H2O
                + 0.99461E-07 OH-
                + 0.99360E-07 H+
                + 0.10057E-09 UO2+)
                ( 298.15 K, 1.0000 atm, aqueous)
                (Eh=-0.201 V, pH= 7.003)

                + 1.0000 mol UO2
                ( 298.15 K, 1.0000 atm, S1, a= 1.0000 )

```

Fig. 8: Gibbs Energy Minimization of UO₂ in one kg of H₂O at 298.15 K for purposes of determining the redox potential.